DOI 10.1007/s11182-015-0441-9

Russian Physics Journal, Vol. 57, No. 12, April, 2015 (Russian Original No. 12, December, 2014)

THE SPECIAL FEATURES OF THE DEFORMATION BEHAVIOR OF AN ULTRAFINE-GRAINED ALUMINUM ALLOY OF THE Al–Mg–Li SYSTEM AT ROOM TEMPERATURE

E. V. Naydenkin, I. P. Mishin, and K. V. Ivanov

UDC 539.52:536.33

The special features of the deformation behavior of an ultrafine-grained aluminum alloy produced by severe plastic deformation are investigated. Unlike ultrafine-grained pure aluminum, the second-phase particles precipitated in the bulk and at the grain boundaries of the alloy are shown to hinder the development of grain boundary sliding and plastic strain localization. This increases the length of the strain hardening stage and uniformity of elongation of a heterogeneous aluminum alloy specimen as compared to pure aluminum.

Keywords: severe plastic deformation, ultrafine-grained structure, aluminum alloy, deformation behavior.

Formation of ultrafine-grained (UFG) structure in metallic materials produced by severe plastic deformation improves the strength properties and concurrently impairs the ductility of the alloys [1, 2]. It has been found in [3] that this is associated with a short strain-hardening stage due to plastic strain localization. As demonstrated with nanostructured electrolytic nickel [4], the relaxation processes responsible for migration of grain boundaries and recrystallization of the material may develop in localized deformation regions. Furthermore, along with formation of localized deformation bands, grain boundary sliding as a high-temperature deformation mechanism may take place even at low temperatures [5]. The particle precipitation at grain boundaries and in the bulk of the grains hinders the development of the foregoing processes and hence improves the ductility of UFG materials [6].

In view of the fact that comprehensive studies on the second-phase particle precipitation effect in heterophase materials are virtually lacking, we set ourselves the task of investigating the deformation behavior of an UFG alloy of the Al–Mg–Li system with Sc and Zn additions (alloy 1421) produced by the equal-channel angular pressing (ECAP) technique. For the sake of comparison, an examination was made of the microstructure and deformation behavior of pure aluminum with UFG structure formed by severe plastic deformation based on ECAP.

THE TEST MATERIAL AND INVESTIGATION TECHNIQUES

The investigations in question were performed on an Al – 5% Mg – 2.2% Li – 0.12% Zr – 0.2% Sc alloy (wt.%) with UFG structure formed by ECAP (12 passes, route B_C at 643 K) [1, 2]. The UFG structure of 99.99% pure aluminum was produced by 8 ECAP passes, route B_C at room temperature. Coupons of dumb-bell tension test pieces with a $5 \times 2.5 \times 1$ mm gage section were removed by the electrospark technique. The specimen surface was subjected to mechanical grinding followed by electrolytic polishing in a 20% $HClO_4$ + 80% CH_3COOH solution. The tensile tests were conducted at room temperature with an initial deformation velocity of 10^{-2} s^{-1}. For comparison purposes, we conducted tensile tests on a hot-rolled alloy in a coarse-grained state with an average grain size of ~20 μm. The microstructure of the material was examined under a Jeol JEM-2100 transmission electron microscope with

Institute of Strength Physics and Materials Science of the Siberian Branch of the Russian Academy of Sciences, Tomsk, Russia, e-mail: nev@ispms.tsc.ru. Translated from Izvestiya Vysshikh Uchebnykh Zavedenii, Fizika, No. 12, pp. 79–82, December, 2014. Original article submitted March 11, 2014; revision submitted September 3, 2014.

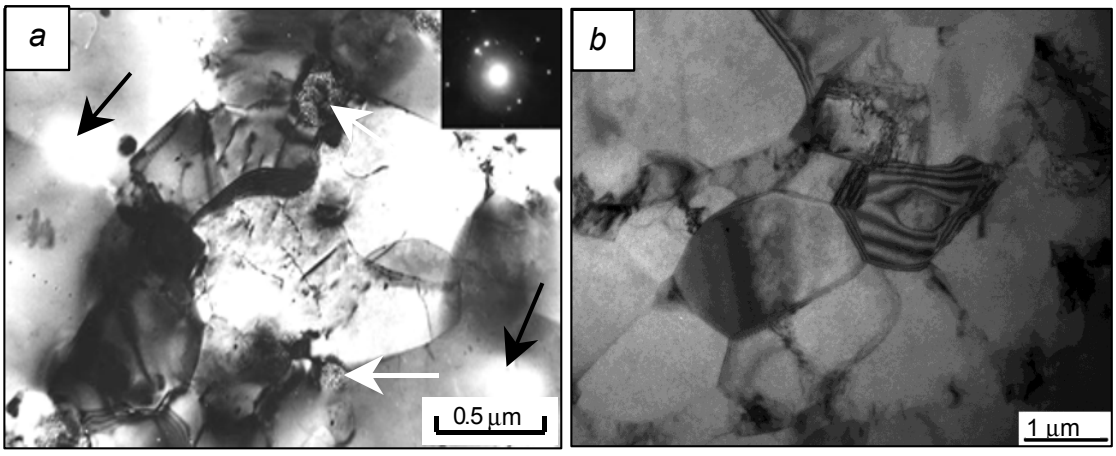

Fig. 1. Microstructure of alloy 1421 (*a*) and pure aluminum (*b*) subjected to ECAP: the *S*-phase particles of complex composition are shown by arrows; dislocations locked by dispersion particles are seen in the central grain.

an accelerating voltage of 200 kV. Foils for electron microscopy were prepared by double-sided jet polishing in a 10% HNO_3 + 90% H_2O electrolytic solution. The strain-induced surface relief of the prepolished specimens subjected to tensile testing was examined under a Carl Zeiss EVO 50 scanning electron microscope.

RESULTS AND DISCUSSION

The microstructure of alloy 1421 and pure aluminum subjected to ECAP is illustrated in Fig. 1. It follows from the data obtained by transmission electron microscopy (Fig. 1) that both of the materials have a close average grain size (1.1 and 1.3 μm, respectively) and the same dislocation density (~10^9 cm^{-2}). However, the alloy exhibits second-phase particle precipitation in the bulk of the grains and at grain boundaries. The structural-phase state of the alloy subjected to severe plastic deformation based on ECAP has been studied extensively in [7, 8] to show that the volume fraction of the grain boundary precipitates (*S*-phase particles) of size 0.3–0.4 μm (Fig. 1*a*) amounts to 3.5%.

Our room-temperature investigations into the mechanical properties and deformation behavior of alloy 1421 of the Al–Mg–Li system with coarse-grained (*d*~10 μm) and UFG structure have revealed that these materials demonstrate higher mechanical characteristics and an essentially different shape of the stress-strain curves as compared to UFG aluminum (Fig. 2). The UFG aluminum structure exhibits a short strain hardening stage (~0.4 %) with a long softening section (>25%) preceding fracture, which is typical for materials produced by severe plastic deformation. Contrastingly, long strain hardening stages (~18 and 13%, respectively) are observed in the stress-strain curves for the coarse-grained and UFG alloys 1421 up to the development of the fracture stage. Notably, the degree of uniform strain corresponding to that found in the alloys at ultimate stress is virtually the same as the prefracture strain (Fig. 2).

Scanning electron microscopy of the strain-induced surface relief has revealed the cause for the short strain-hardening stage in pure UFG aluminum. This is plastic strain localization at the macroscopic level observed as early as the onset of the plastic flow responsible for the neck formation at ultimate stress (Fig. 3*a*), which decreases uniform specimen elongation corresponding to the plastic strain at ultimate stress [9]. Once the ultimate stress is attained, the UFG aluminum specimens undergo strain in the neck alone as evidenced by the absence of elongation of the circles marked on the gage length outside of the neck before straining the specimens (Fig. 3*a*). The basic plastic deformation modes in the neck region of the UFG aluminum specimens are mesoscale cooperative grain boundary sliding (relative displacement of several grains), whose contribution to the total deformation increases, and localized deformation bands (Fig. 3*a*). The relaxation mechanism of grain boundary migration favorable for the grain growth is found to develop in the localized deformation bands of the UFG aluminum specimens [9].

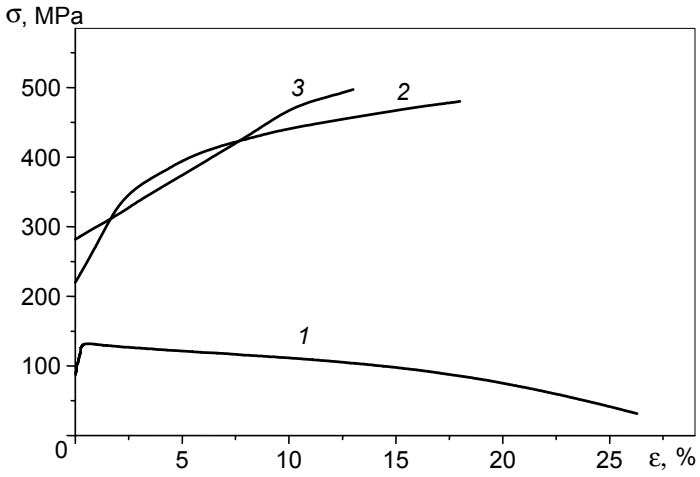

Fig. 2. True stress-true strain curves for tensile UFG aluminum (curve *1*), alloy 1421 (curve *3*), and coarse-grained alloy specimens (curve *2*) at 295 K.

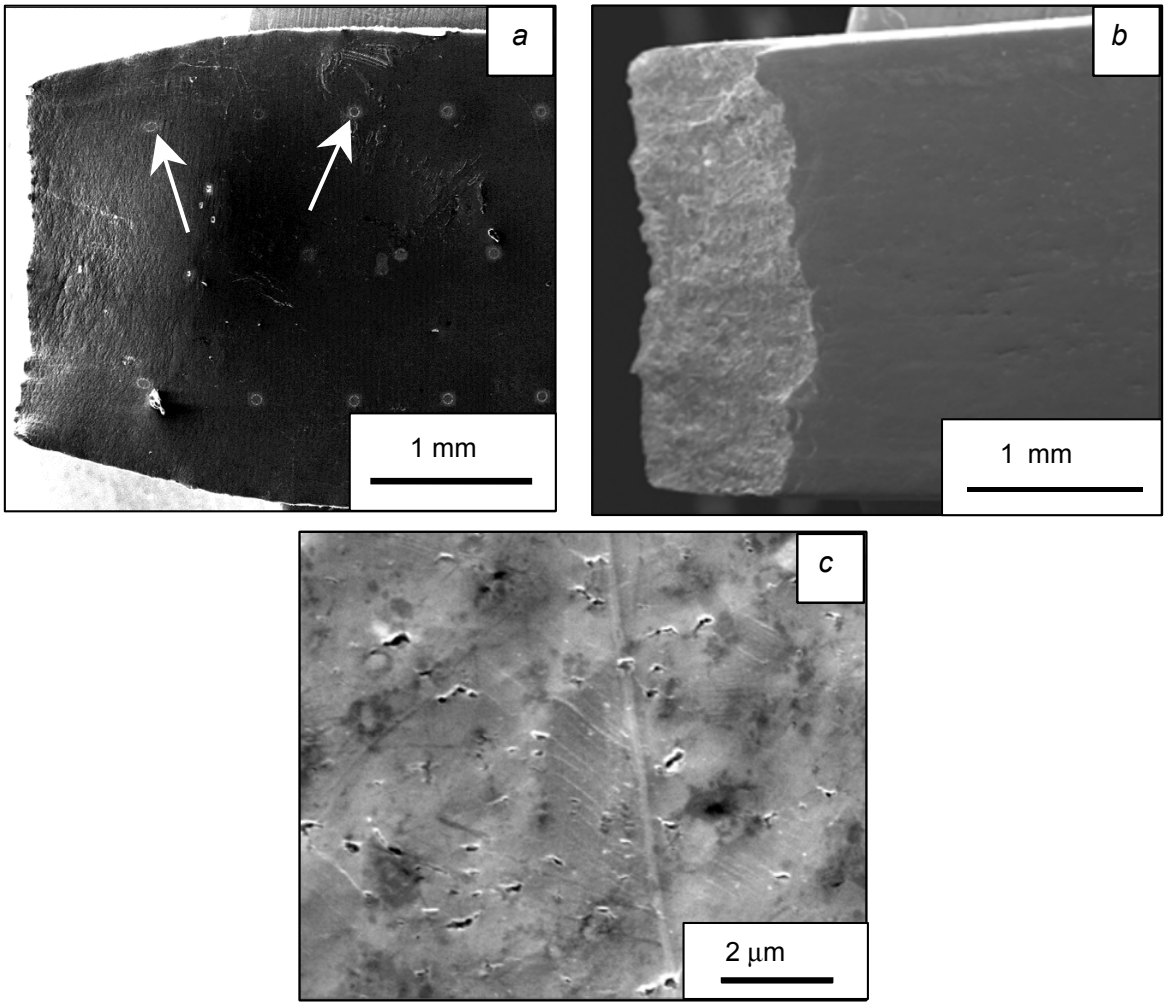

Fig. 3. Lateral faces of the UFG aluminum (*a*) and alloy 1421 specimens (*b* and *c*) subjected to room-temperature tension. The arrows show circles marked on the surface of the UFG aluminum specimen (*a*).

Unlike UFG aluminum, the alloy 1421 specimens both in the coarse-grained and in the UFG states demonstrate more uniform deformation along the gage length of the test pieces without distinct necking (Fig. 3*b*). In large grains, microscale plastic deformation develops by intragrain dislocation gliding (Fig. 3*c*). At the same time, the second-phase particle precipitation at the grain boundaries and in the bulk of the grains efficiently hinders the transition of deformation to the mesoscale level and development of grain boundary migration, grain boundary sliding, and localized deformation bands (Fig. 3*b*). This is evident in the absence of plastic deformation steps at the grain boundaries in the strain-induced surface relief, which is characteristic of this plastic deformation mechanism, and of localized deformation bands (Fig. 3). An analysis of the fracture patterns of the materials under study has revealed that the UFG aluminum specimens exhibit tough fracture, whereas the alloy 1421 test pieces are characterized by brittle-tough fracture irrespective of their structure.

CONCLUDING REMARKS

We have investigated the special features of the deformation behavior of an ultrafine-grained aluminum alloy produced by the severe plastic deformation technique. It has been found that with comparable characteristics of the ultrafine-grained structure (average grain size and dislocation density), the deformation behavior of the Al – 5% Mg – 2.2% Li – 0.12% Zr – 0.2% Sc alloy (wt.%) at room temperature essentially differs from that of pure aluminum. This is evident in a longer strain-hardening stage and absence of macroscale plastic strain localization due to neck formation. The difference arises from precipitation of fine intermetallic phase particles in the bulk of the grains, which favors an increase in the length of the strain-hardening stage, and of *S*-phase particles at the grain boundaries, increasing the resistance of the material to the development of grain boundary sliding and macroscale strain localization.

The work was financed by the Siberian Branch of the Russian Academy of Sciences within the Budgetary Support Project № III.23.2.2. Examination of the strain-induced surface relief of coarse- and ultrafine-grained Al–Mg–Li–Zr–Sc alloys under a scanning electron microscope was supported by the Ministry of Education and Science of the Russian Federation (Agreement № 02.G25.31.0063) in the framework of the implementation of Resolution № 218 of the RF Government.

REFERENCES

1. R. Z. Valiev and I. V. Alexandrov, Bulk Nanostructured Metallic Materials: Production, Structure, and Properties [in Russian], IKTs Akademkniga, Moscow (2007).
2. Yu. R. Kolobov, R. Z. Valiev, G. P. Grabovetskaya, *et al.*, The Grain Boundary Diffusion and Properties of Nanostructured Materials [in Russian], Novosibirsk, Moscow (2001).
3. E. V. Naydenkin and G. P. Grabovetskaya, Mater. Sci. Forum, **633**–**634**, 107–119 (2010).
4. K. V. Ivanov and E. V. Naydenkin, Scripta Mater., **66**, 511–514 (2012).
5. F. Dalla Torre, H. Van Swygenhoven, and M. Victoria, Acta Mater., **51**, 3957–3970 (2002).
6. E. Ma, Scripta Mater., **49**, 663–668 (2003).
7. Yu. R. Kolobov, E. V. Naidenkin, E. F. Dudarev, *et al.*, Russ. Phys. J., **45**, No. 5, 453–457 (2002).
8. E. V. Naidenkin, Yu. R. Kolobov, E. F. Dudarev, and I. P. Mishin, Fiz. Mezomekh., No. 8, Sp. Iss., 71–75 (2005).
9. K. V. Ivanov and E. V. Naidenkin, Mater. Sci. Forum, **667**–**669**, 915–920 (2011).